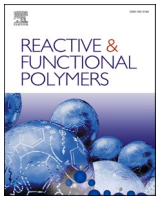
Reactive and Functional Polymers 216 (2025) 106445



Contents lists available at ScienceDirect

Reactive and Functional Polymers

journal homepage: www.elsevier.com/locate/react





Tuning the properties of gelatin films through crosslinking and addition of ionic liquids

Alaitz Etxabide [a], Estela O. Carvalho [b,c,g], Nelson Pereira [b,g], Daniela Correia [d], Pedro Guerrero [a,e,*], Carlos M. Costa [b,g], Koro de la Caba [a,e,*], Senentxu Lanceros-Mendez [b,e,f]

[a] BIOMAT research group, University of the Basque Country (UPV/EHU), Engineering College of Gipuzkoa, Plaza de Europa 1, 20018 Donostia-San Sebastián, Spain
[b] Physics Centre of Minho and Porto Universities (CF-UM-UP) and Laboratory of Physics for Materials and Emergent Technologies, LapMET, University of Minho, 4710-057 Braga, Portugal
[c] Centre of Biological Engineering (CEB), University of Minho, Campus de Gualtar, Braga 4710-057, Portugal
[d] Center of Chemistry, University of Minho, 4710-057 Braga, Portugal
[e] BCMaterials, Basque Center for Materials, Applications and Nanostructures, UPV/EHU Science Park, 48940 Leioa, Spain
[f] Ikerbasque, Basque Foundation for Science, 48009 Bilbao, Spain
[g] Institute of Science and Innovation for Bio-Sustainability (IB-S), University of Minho, 4710-053 Braga, Portugal

ARTICLE INFO

Keywords:
Gelatin
Ionic liquids
Films
Crosslinking

ABSTRACT

The exploration into biopolymer applications has experienced fast growth in recent years due to the ever-growing environmental and societal demand for a greener and safer environment. In this study, fish gelatin-based films with fructose and different choline-based ionic liquids, such as choline dihydrogen phosphate, choline acetate, and choline serinate, were prepared to assess the effect of Maillard reaction and the inluence of the ionic liquids on the film properties. Overall, the presence of physical and chemical interactions enhanced UV–Vis light absorption capacity, reduced the solubility, improved film flexibility and conductivity. These changes were related to the formation of Maillard reaction products, the plasticising effect of ionic liquids and the increase in ionic mobile species associated with the ionic liquids within the films. This study shows the possibility of tailoring the properties of bio-based materials via Maillard reaction and the addition of ionic liquids.

1. Introduction

In recent years, the exploration into biopolymer applications is experiencing fast growth with the main aim of replacing the synthetic and non-biodegradable polymers obtained from finite petroleum resources, a transition stemmed from the ever-growing societal demand for a more sustainable and safer environment [1]. Biopolymers are biodegradable, biocompatible and environmentally friendly, and they possess tunable physicochemical properties which make these materials attractive and promising for the replacement of conventional polymers in many applications, for instance, food, medical and pharmaceutical-related use [2]. Among them, fish gelatin has been considered a promising biopolymer for the development of sustainable materials.

Fish gelatin, a protein obtained from the hydrolysis of collagen, is extracted from marine waste and so, it is a renewable, economical and abundant biopolymer. In addition, this protein has excellent film-forming capacity, transparency and barrier properties to both UV light and oxygen [3]. However, some characteristics, such as stability in contact with aqueous liquids and mechanical properties, are to be improved to extend the applicability of the material [4]. Different strategies have been employed to modify/tailor the properties of gelatin. For instance, the use of additives such as plasticizers (glycerol is the most employed one), bio-nano-reinforcements (mainly made of cellulose), crosslinkers and, more recently, ionic liquids (ILs), has been reported [5–7].

The use of crosslinkers is necessary to improve the stability of hydrophilic materials in aqueous solutions. Therefore, their employment has become essential to improve gelatin-based materials' behaviour when they are in contact with water. Among crosslinkers, glutaraldehyde (cytotoxic issues), genipin (less toxic than aldehydes), photo-crosslinkers (e.g. riboflavin or vitamin B_2) and sugars (e.g. ribose, fructose, lactose) have been used as crosslinking agents for their ability

* Corresponding authors.
E-mail addresses: pedromanuel.guerrero@ehu.es (P. Guerrero), koro.delacaba@ehu.es (K. de la Caba).

https://doi.org/10.1016/j.reactfunctpolym.2025.106445
Received 26 March 2025; Received in revised form 21 July 2025; Accepted 7 August 2025
Available online 8 August 2025
1381-5148/© 2025 The Authors. Published by Elsevier B.V. This is an open access article under the CC BY-NC-ND license (http://creativecommons.org/licenses/by-nc-nd/4.0/).

Table 1
Nomenclature used to identify the gelatin-based films prepared in this study as a function of added ionic liquid (ChDHP, ChSer, ChAc), pH (5.4, 10) and heat treatment (non-heated (NH), heat-treated HT).

Films	ILs	pH
C5.4 NH	–	5.4
C10 NH	–	10
ChDHP NH	[Ch][DHP]	5.4
ChSer NH	[Ch][Ser]	10
ChAc NH	[Ch][Ac]	10
C5.4 HT	–	5.4
C10 HT	–	10
ChDHP HT	[Ch][DHP]	5.4
ChSer HT	[Ch][Ser]	10
ChAc HT	[Ch][Ac]	10

to react with gelatin [8–10]. In the case of sugars, their interactions with proteins occur through a process called Maillard reaction (MR), a non-enzymatic browning reaction that chemically links protein chains [11,12].

Other agents that also can interact with gelatin are ILs. ILs are completely composed of ions and so, the interactions between proteins and ILs may occur via different anionic, cationic, hydrophobic, and polar interactions from each amino acid of a protein backbone with the cation and anion available in the ILs [5,13]. By appropriate selection of different combinations of anions and cations, the physicochemical properties (e.g., elongation at break, hydrophobicity and solubility), as well as electrical characteristics (e.g. ionic conductivity) of IL-containing biopolymers can be tailored [14–16]. Among ILs, choline [Ch]-based ILs have received the most attention in recent years, since they possess beneficial properties such as non-toxicity and biodegradability [17].

In contrast to what has been evaluated so far, where MR [8,11,12] and the addition of ILs [5,15] on gelatin films have been studied separately, in this work, the effect of the addition of fructose and/or different [Ch]-based ILs on the physical and chemical crosslinking of gelatin-based films and, thus, on their final properties has been assessed. For that, optical, barrier, physicochemical, morphological, mechanical, antimicrobial and cytotoxicity properties have been studied to understand the additives' effect on films' properties for different applications. As far as the authors know, no previous research has investigated the combined effect of Maillard reaction and [Ch]-based ILs addition on gelatin films' properties which could open up new paths for tailoring bio-based materials for wider and unexplored applications.

2. Materials and methods

2.1. Materials

Type A fish gelatin (Weishardt International), with 200 Bloom (gel strength), 11.06 % moisture and 0.147 % ash content, was used as a matrix. D(−)-fructose (VWR Chemicals BDH®, USA) was employed as a crosslinker. Various ILs (**Fig. S1**), such as choline dihydrogen phosphate [Ch][DHP] (> 98 %, powder), choline acetate [Ch][Ac] (> 98 %, powder) and choline serinate [Ch][Ser] (> 95 %, yellowish liquid, 60 % in H_2O) were supplied by Ionic Liquids Technologies GmbH and, were used to modify films' functionalities. NaOH 1 M was used to modify the pH of the film forming solutions and distilled water was used as a solvent.

2.2. Film preparation

Films were prepared via the solution-casting method. First, 2.5 g gelatin and 20 wt% of fructose (on a gelatin dry weight basis) were dissolved in 50 mL water at 60 °C and 250 rpm for 30 min. Then, 10 wt% of IL (on a gelatin dry weight basis) was added and the pH of the solution was modified to 10 in [Ch][Ac]- and [Ch][Ser]-containing solutions to foster the MR while pH (5.4) was not changed in [Ch][DHP]-containing solution to avoid [Ch][DHP] precipitating while film drying. The resulting solutions were maintained at 60 °C for 30 min under stirring before 4.5 g of the solutions were poured into Petri dishes (ø 60 mm), which were then left to dry at 37 °C for 24 h in an oven (VENTICELL ECO line, MMM Group, Germany). Finally, the films were peeled off and some of them were heated at 80 °C for 24 h to obtain heat-treated (HT) films. Non-heated films were designated as NH films. Control films (C) were also prepared following the above-mentioned procedure at both pHs (5.4 and 10) but without the addition of ILs. The designation of the films is summarized in Table 1. Films with an average thickness of 87 μm were obtained.

2.3. Film characterization

2.3.1. Optical and barrier properties

The colour of the films was determined with the CR-400 Minolta Chroma Meter colourimeter (Konika Minolta, Spain). Films were placed on the surface of a white standard plate (calibration values: L* = 97.39, a* = 0.03, b* = 1.77) and colour parameters were measured using the CIELAB colour scale: L* = 0 (black) to L* = 100 (white), −a* (greenness) to +a* (redness), and –b* (blueness) to +b* (yellowness). Fifteen measurements ($n = 15$) were taken for each composition.

Light barrier properties of the films were assessed using a UV Multiskan ultraviolet-visible (UV–Vis) spectrophotometer (SkyHigh, Spain). The light absorbance of films from 200 to 800 nm was measured. Three specimens were tested for each composition ($n = 3$).

Water vapour permeability of the films was measured using a PERME™ W3/0120 instrument (Labthink, China) to determine WVP gravimetrically ($n = 2$) at 38 °C and 90 % relative humidity, according to ASTM E96–00. Water vapour permeability (WVP) was determined using Eq. 1:

$$\mathbf{WVTR}\left(\frac{\mathbf{g}}{\mathbf{m^2 \bullet day}}\right) = \frac{\mathbf{G}}{\mathbf{t \times A}} \quad (1)$$

where G is the weight change, t is time and A is the test area.

2.3.2. Vibrational spectra, crystallinity and morphological evaluation

Gelatin films were assessed using Fourier transform infrared (FTIR) spectroscopy (Bruker ALPHA II FTIR spectrometer, Spain), equipped with attenuated total reflectance (ATR) crystal. A total of 32 scans were performed at 4 cm^{-1} resolution and the measurements were recorded between 4000 and 750 cm^{-1}. Three measurements ($n = 3$) were taken for each composition.

The amorphous/crystalline character of gelatin films was assessed using Xpert Pro X-ray diffraction (XRD) equipment (PANalytic, Spain) with Cu-Kα (λ = 1.5418 Å) as a radiation source. The analysis was carried out at 40 kV and 40 mA from 2θ = 5 to 50°.

The film microstructure was assessed using a Hitachi S-4800 scanning electron microscope (SEM Hitachi, Spain) with an acceleration voltage of 5.0 kV to visualise the film surface and cross-section. For that, the films were cut, placed on a metallic stub, and coated with gold under vacuum in an argon atmosphere.

2.3.3. Mechanical properties

Tensile tests were carried out to measure the tensile strength (TS) and elongation at break (EB) of the films with a Texturometre TA.XT plusC (Stable Microsystems, Spain), according to ASTM D882–02. Films were cut into bone-shaped samples (4.75 mm × 22.25 mm), and the tensile test was conducted with a load cell of 50 N and a crosshead rate of 5 mm/min. Four samples were measured for each system ($n = 4$).

2.3.4. Electrical properties

To determine the electrical conductivity of the films, first, the sam-

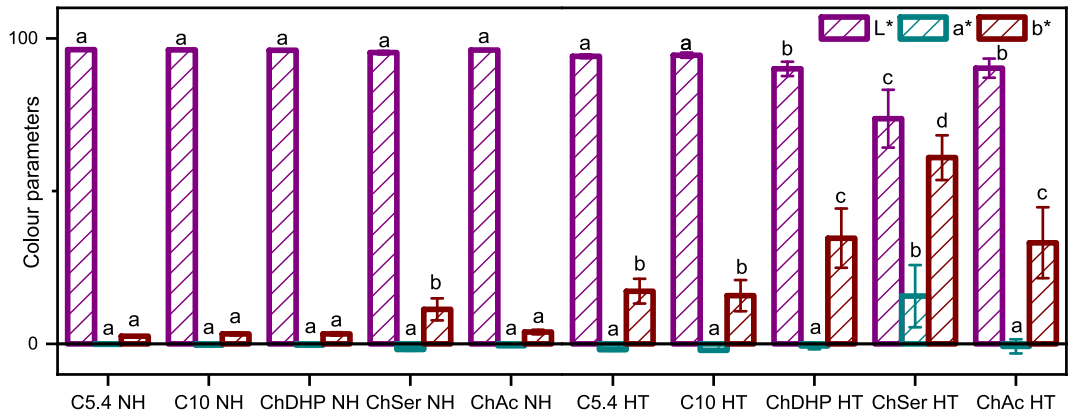


Fig. 1. L*, a* and b* colour parameters of gelatin films as a function of pH (5.4 and 10), the addition of ionic liquids ([Ch][DHP], [Ch][Ser] and [Ch][Ac]) and heat treatment (non-heated (NH) and heat-treated (HT)). Means that do not share a letter (a, b, c) are significantly ($p < 0.05$) different ($n = 15$).

ples were coated with Polaron sputter coater SC502 of gold on both sides on 5 mm diameter electrodes in a parallel configuration and then, the characteristic I—V curves were obtained using a Keithley 487 picoammeter/voltage source (Keithley, Spain) at room temperature with an applied voltage between ±10 V. Eq. 2 was used to calculate the conductivity of the films:

$$\sigma\left(\frac{S}{cm}\right) = \frac{d}{R \times A} \tag{2}$$

where d is the thickness, R is the resistance of the sample and A is the electrode area.

The bending response of the actuators was evaluated using an Agilent 33220 A function generator and a PicoScope 4227 oscilloscope in samples with dimensions of 12 mm × 2 mm × 87 μm. Previous to the measure, gold electrodes with dimensions 12 mm × 2 mm were deposited on both sides of the sample by sputtering technique with a Polaron coater SC502 system. A square-wave signal with a peak voltage of 10 Vpp was applied at a frequency of 100 mHz to the coated strip samples. After analysing all samples, as ChAc10HT showed the highest electrical conductivity, films with different [Ch][Ac] concentrations (10, 20 and 40 wt%) were also prepared to assess the bending response dependence on sample conductivity.

2.3.5. Solubility and water uptake

Solubility and water uptake properties of films (2 cm × 2 cm) were measured by immersing the previously weighed films (W_0) into water (7.5 mL) at 23 ± 2 °C for 24 h. Then, the wet films were taken out from the water, reweighed (W_w) and left to dry at 37 °C for 24 h before carrying out the final weighing of the dry films (W_f). Three specimens ($n = 3$) of each film were tested. The solubility (S) and water uptake (WU) of films were calculated using Eq. 3 and Eq. 4 respectively:

$$S\ (\%) = \frac{W_0 - W_f}{W_0} \times 100 \tag{3}$$

$$WU\ (\%) = \frac{W_w - W_0}{W_0} \times 100 \tag{4}$$

After immersion, to analyse the release of components from the films, water was analysed using various techniques: i) UV–Vis spectroscopy from 200 to 600 nm, ii) conductivity (Universal Multi-Parameter Handheld ProfiLine Multi 3320 – WTW, Germany), and iii) pH meter (HI 5221, Hanna, Woonsocket, USA). Three measurements ($n = 3$) were carried out for each technique and film composition.

Additionally, the previously weighed films (W_0) were immersed in PBS at 37 °C for 24 h. Then, wet films were taken out from PBS, rinsed 3 times in chilled distilled water (4 °C) and left to dry at 37 °C for 24 h before reweighing (W_f). Three specimens (n = 3) of each film were tested. The solubility (S) of films in PBS was also calculated using Eq. 3.

2.3.6. Antimicrobial activity

The antimicrobial activity of films was evaluated using a modified version of the standard shake flask method (ASTM-E2149–01). Gram-positive *Staphylococcus aureus* (*S. aureus*, ATCC 25923) and Gram-negative *Escherichia coli* (*E. coli*, ATCC 25922), purchased from American Type Culture Collection (LGC Standards S.L.U, Spain), were used in the microbial assay. Two bacterial pre-inoculums were obtained by resuspending a single colony from the matching stock bacterial culture in nutrient broth (NB) and culturing it overnight at 37 °C and 110 rpm. Then, bacterial cells in the pre-inoculums were harvested twice by centrifugation at 5000 rpm for 5 min and resuspended in a 0.9 % NaCl (*w/v*) solution. The culture's optical density (OD) was measured at 600 nm and adjusted to 0.1, yielding a workable inoculum of approximately 1×10^6 CFU/mL. Simultaneously, pieces of the samples (1 cm × 1 cm × 87 μm) were sterilized with UV light. The bacterial solution and samples were placed in contact at 37 °C and 200 rpm for 2 h. Finally, the resulting suspensions were serially diluted in sterile 0.9 % NaCl (w/v) solution, plated on plate count NB agar and incubated at 37 °C for 24 h to assess the number of bacteria that survived. This method allows quantitative data for calculating the decrease in the number of colonies formed by comparison with free-floating bacteria under control conditions (without material).

2.3.7. Citotoxicity

The cytotoxicity of PBS-non-soluble films (ChSer10HT and ChAc10HT) was evaluated following the ISO10993-5 standard test method, using the fibroblast L929 cell line. L929 fibroblasts were cultured in a 75 cm^2 cell culture flask using a culture media containing 4.5 g/L glucose supplemented with 10 % Fetal Bovine Serum (FBS, Biochrom) and 1 % Penicillin/Streptomycin (P/S, Biochrom). The flask was incubated at 37 °C and 5 % CO_2 in a humidified atmosphere. The culture media was changed every two days till the confluence reached 60–70 % and, finally, cells were collected using trypsin-EDTA (Biochrom).

To perform the cytotoxicity assessment, 13 mm diameter circles of each system were previously cut and sterilized (UV light for 30 min on each side). Then, samples were placed in a 24-well tissue culture plate containing the previously specified culture media and cultured for 24 h at the same temperature and humidity conditions previously mentioned. Furthermore, as negative and positive controls, 20 % (*v*/v) dimethyl sulfoxide (DMSO, Sigma Aldrich, Portugal) and cell culture media without samples were utilized. Simultaneously, L929 cells were plated in a 96-well tissue culture plate at a density of 3×10^4 cells/mL and cultured in the same conditions for 24 h. Then, the culture media on the 96-well plate was substituted with the medium in contact with the

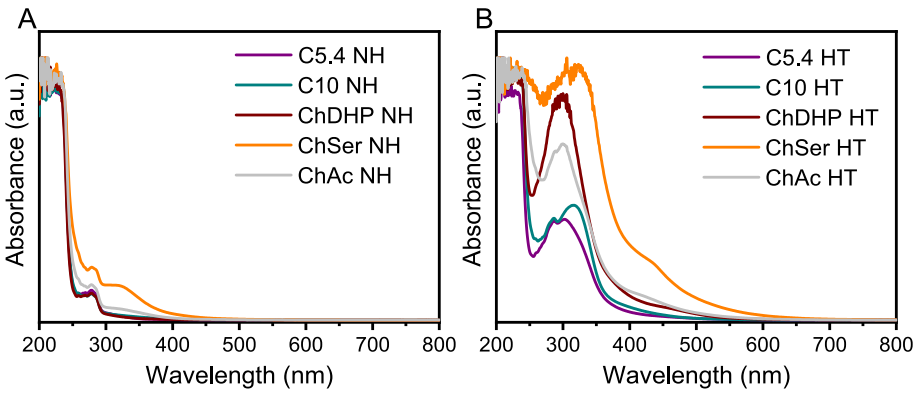


Fig. 2. UV–Vis spectra for A) non-heated (NH) and B) heat-treated (HT) gelatin films as a function of pH (5.4 and 10) and addition of ionic liquids ([Ch][DHP], [Ch][Ser] and [Ch][Ac]) ($n = 3$).

samples, and the plate was left to incubate for 72 h. At that time, the indirect cell viability was evaluated using a 3-(4,5-dimethylthiazol-2-yl)-2,5-diphenyltetrazolium bromide (MTT) assay. After removing the media, a fresh medium containing 10 % MTT solution was added and incubated for 3 h. The produced MTT crystals were dissolved in DMSO, and the optical density at 570 nm was determined using a microplate reader (Biotech Synergy HT, Winooski, VT, USA). The MTT test measures live cells by converting MTT into a purple-coloured formazan crystal that is dissolved in DMSO.

2.4. Statistical analysis

Data were subjected to a one-way analysis of variance (ANOVA) through an SPSS computer program (SPSS Statistic 25.0). Post hoc multiple comparisons were determined by Tukey's test with the level of significance set at $p \leq 0.05$.

3. Results and discussion

3.1. Optical and barrier properties

The colour of the films was measured to assess the effect of IL addition, pH and heat treatment on the film appearance (Fig. 1). Neither the increase in pH (from 5.4 to 10) nor the addition of [Ch][DHP] and [Ch][Ac] ILs had a significant effect on NH films' colour. The addition of [Ch][Ser] decreased the a* and increased the b* parameters, making films greener and yellower due to the yellow colour of [Ch][Ser] ionic liquid solution. Regarding the heat treatment, the control films (C5.4 HT and C10 HT) became more yellowish/brownish. The development of pale and dark colours in heated control films is the visible result of the Maillard reaction (MR). As for the addition of ILs in HT films, with the presence of [Ch][DHP] and [Ch][Ac], b* increased further than in HT control films, while L* decreased. Regarding [Ch][Ser]-containing films, IL addition further decreased L*, while a* and b* values notably increased. These results indicated that higher browning occurred in the presence of ILs, especially when [Ch][Ser] was added. As the crosslinking extension can be indirectly assessed through colour measurements [18], the higher browning in ChSer HT samples could be indicative of a higher crosslinking degree in [Ch][Ser]-containing HT films than in the other HT samples, which may be attributed to the greater interaction with ILs due to the amino groups in the IL participated in the MR.

Regarding films' light barrier properties (Fig. 2), all NH films exhibited a high UV light absorption capacity in the 200–300 nm range, regardless of the pH and added ILs, due to the presence of peptide bonds (200–250 nm) and chromophores (e.g., tyrosine and phenylalanine) (250–300 nm) in gelatin. It was observed that the addition of [Ch][Ser], a coloured IL, increased the UV light absorbance capacity of films up to

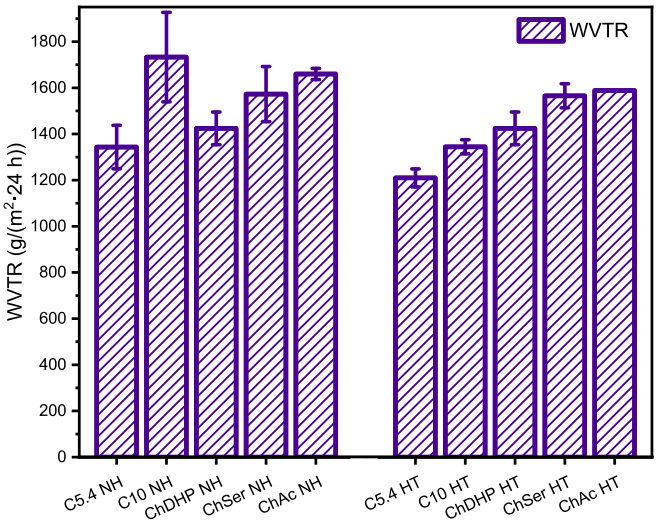


Fig. 3. Water vapour transmission rate (WVTR) values for gelatin films as a function of pH (5.4 and 10), addition of ionic liquids ([Ch][DHP], [Ch][Ser] and [Ch][Ac]) and heat treatment (non-heated (NH) and heat-treated (HT)) ($n = 2$).

380 nm and, to a lesser extent, in the Vis region (> 380 nm). This could be because [Ch][Ser] is a choline-based amino acid IL with a yellowish colour. This latter outcome goes in line with the increase in the b* parameter observed in Fig. 1 for ChSer NH films. As for the heat treatment, an increase in UV–Vis light absorption in all HT films was observed, which was related to the MR. The increase in pH from 5.4 to 10 improved the light barrier properties of the films (C10 HT), indirectly related to a more extended crosslinking reaction, as observed in our previous works [11,18]. As for the IL addition, the light absorbance capacity of the films considerably increased, being the ChSer HT films the samples with the best light barrier properties. This latter observation indicated that a more extended MR occurred in ChSer HT films, as above indicated (Fig. 1), and this could be because [Ch][Ser] is an amino acid IL that could also react with fructose via MR. The increase in absorbance in the UV region could provide films with a preventive (secondary) antioxidant function [19], an interesting characteristic for both food- and biomedical-related applications.

In the same manner, the WVTR values (Fig. 3), in the range of 1200–1700 $g \cdot m^{-2} \cdot day^{-1}$, provide these films with suitable properties for both food packaging and biomedical applications. Further, WVTR values are similar to those of polymer-based membranes with medium-permeability (2028.3 ± 237.8 $g/m^{-2} \cdot day^{-1}$), which have demonstrated a more rapid wound healing in mouse models than low

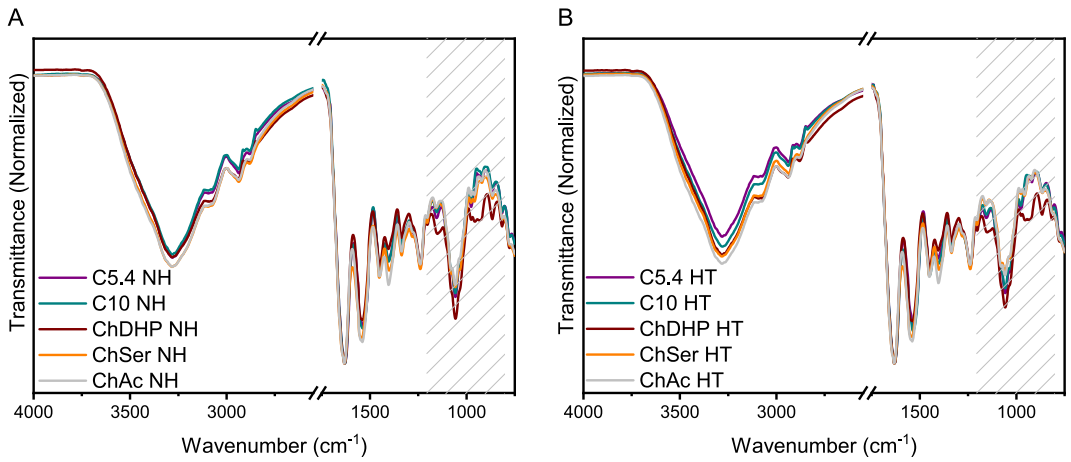


Fig. 4. FTIR spectra for A) non-heated (NH) and B) heat-treated (HT) gelatin films as a function of pH (5.4 and 10) and addition of ionic liquids ([Ch][DHP], [Ch][Ser] and [Ch][Ac]) ($n = 3$).

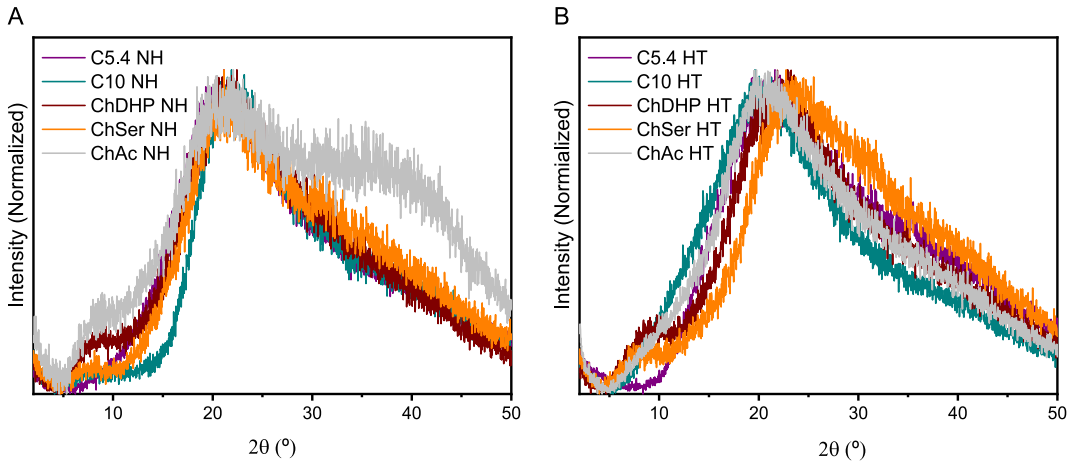


Fig. 5. XRD patterns for A) non-heated (NH) and B) heat-treated (HT) gelatin films as a function of pH (5.4 and 10) and addition of ionic liquids ([Ch][DHP], [Ch][Ser] and [Ch][Ac]). The peak intensity carries the same value due to the normalized diffractogram.

permeability membranes (954.8 g^{-2}·day^{-1}) [20,21]. On the other hand, these films displayed permeability values akin to standard packaging materials for bakery products [22]. Among the studied variables (pH, IL addition and heat treatment), it could be stated that the addition of [Ch]-based ILs had the greatest impact on the water barrier properties of the films. The increase in the permeability of the films has been related to an overall crystallinity reduction, and the plasticiser effect of ILs [23].

3.2. Physicochemical and morphological properties

The FTIR analysis of individual components can be found in the supplementary data (**Fig. S2**). Regarding the films (Fig. 4), all samples exhibited the characteristic vibration bands of gelatin, amide A (3277 cm^{-1}), amide I (1627 cm^{-1}), amide II (1528 cm^{-1}), and amide III (1237 cm^{-1}), while [Ch][DHP]-containing films showed vibration bands corresponding to -P=O and -P-OH bonds in the 1050–950 cm^{-1} range [24]. The addition of ILs and the heat treatment induced clear shifts in the main bands of gelatin (**Table S1**), related to physical interactions (e.g., H-bonding and electrostatic interactions) and Maillard reaction (mainly observed in the patterned area in Fig. 4 A and B), respectively [5,25–27]. Therefore, it can be stated that ILs promote physical interactions with gelatin, while the heat treatment induces the formation of MR products via a chemical reaction.

Regarding the structure of gelatin, the C5.4 NH film showed two characteristic diffraction bands at $2\theta \approx 7.5°$ and 21° (Fig. 5). The band at $2\theta \approx 7.5°$ is correlated with the triple-helix in gelatin film since triple-helix structures were reformed during the film drying [28]. As for the broad diffraction band at 21°, this is related to the partial crystalline structure of gelatin, as opposed to an irregular arrangement (amorphous) of gelatin macromolecule chains [29]. Fig. 5 shows a decrease in the intensity of this band when pH modification (from pH 5.4 to pH 10), the addition of ILs and the heat treatment were carried out, which could be related to a disruption of non-covalent interactions (hydrogen bonding, hydrophobic interactions, charge attractions and repulsions) due to the modifications in the formulation and the processing conditions, which led to a decrease in films' crystallinity. This decrease could be attributed to the disruption of physical interactions due to: i) the basic pH [30]; ii) the plasticization effect of IL [31,32]; and iii) the formation of cross-links and glyco-conjugates during MR promoted by the heat treatment [33]. The crystallinity reduction could be related to an increase in the permeability of the films (Fig. 3), as previously explained.

Regarding film morphology, Fig. 6 shows the SEM images of the surface and cross-section of HT films since there was no difference between NH and HT films. As can be observed, films showed dense and homogeneous structures with no visible voids, cracks and/or agglomerates. These results indicated that all the film-forming components were homogeneously mixed due to their water-solubility and/or dispersion properties. Similar results were observed in biopolymer-based structures using biocompatible [Ch]-based ionic liquids [34,35].

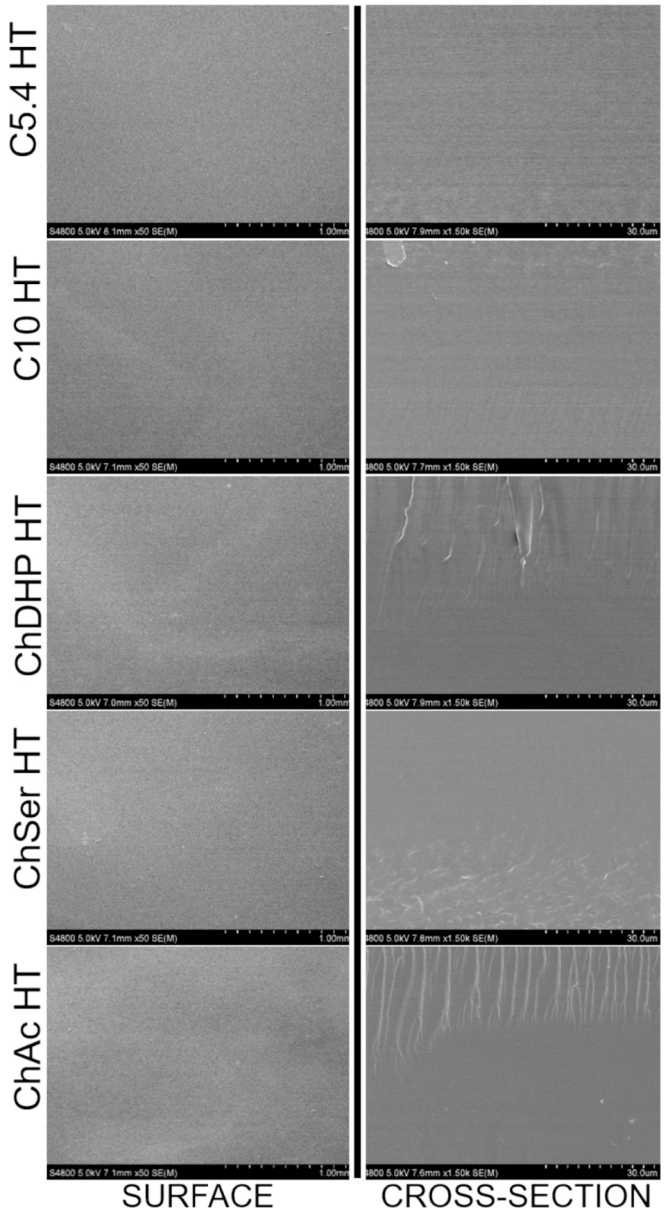


Fig. 6. SEM images (surface and cross-section) of heat-treated (HT) gelatin films as a function of pH (5.4 and 10) and addition of ionic liquids ([Ch][DHP], [Ch][Ser] and [Ch][Ac]). Bar scales (at the right bottom of each image are constructed with 11 short lines) for surface and cross-sections were 1.00 mm and 30.0 μm, respectively.

3.3. Mechanical properties

The mechanical properties of gelatin-based films were notably affected by the addition of ILs and to a lesser extent by MR (**Fig. S3**). With the addition of ILs, tensile strength (TS) values of films significantly decreased (Fig. 7A) while elongation at break (EB) notably increased (Fig. 7B). The same behaviour was also observed in other biopolymer-based materials when ILs were added [36]. For instance, upon the addition of choline citrate IL to gelatin, the elongation at break increased to approximately 460 % from around 7 % [37]. This result was related to the plasticizing effect of choline citrate on the gelatin matrix. Therefore, [Ch]-based ILs used in the current study could behave as plasticizers and induce flexibility in gelatin films.

3.4. Electrical properties

The electrical properties of the films were significantly enhanced when ILs were added to the film formulation (Fig. 8), especially when [Ch][Ac] was used. These latter films showed conductivity values of around 6.22×10^{-8} S/cm and 7.76×10^{-8} S/cm, for ChAc NH and ChAc HT samples, respectively, two orders of magnitude larger than the control gelatin films. As explained by Andonegi and co-workers [38], when assessing collagen-based composites with ILs, the increase in conductivity was related to the increase in the number of ionic mobile species associated with the IL. It was also found that the heat treatment slightly assisted in the ionic conductivity enhancement of the system.

Concerning bending actuator response, none of the samples showed any bending response (data not shown). As it depends on IL content [39], HT films with higher amounts of [Ch][Ac] were prepared and the bending response of those films was assessed (**Fig. S4**). Unlike 10 % and 20 % [Ch][Ac]-containing HT films, samples with 40 % [Ch][Ac] showed a bending response of 9 mm, at a voltage of 10Vpp in 10 s, which is attributed to the movement of the anions in the positive electrode layers and the cations in the opposite layer. The overall bending characteristics are dependent on the suitable combination of mechanical and electrical properties [40]. Further assessments of these formulations with higher [Ch][Ac] amounts were not carried out in this work.

3.5. Solubility and water uptake

The assessment of films' water uptake and solubility in contact with water is another indirect way to analyse the effect of IL addition and MR on the gelatin films since the presence of interactions can affect the water stability of materials. Unlike control NH and ChDHP NH films (Fig. 9 A and B), ChSer NH and ChAc NH films were not soluble in water at 23 °C and were able to uptake water within their structure (~1000 %). Considering that gelatin is water-soluble, the results of ChSer NH and ChAc NH films indicated that there were stable interactions between gelatin and these ILs, which made the film non-water soluble. These results went in line with the FTIR outcomes (Fig. 4) and are attributed to the interaction between IL and gelatin structure. As for the heat treatment and pH effect on the films' water stability behaviour, the combination of pH increase up to 10 and the MR induced by the heat treatment improved the stability since films became less water soluble than their NH counterpart.

The above results reinforced optical, light barrier and FTIR outcomes which all indicated that; I) physical interactions occurred between gelatin and [Ch][Ac] and [Ch][Ser] ILs in NH fims; II) heat-treatment induced the MR between gelatin and fructose in control HT films; and III) the presence of ILs, especially the [Ch][Ser] IL, further promoted interactions with gelatin in IL-containing HT films.

The analysis of the remaining water after the solubility test (Fig. 9 C and D) showed that both the pH and conductivity of the liquid varied depending on the pH, type of IL and heat treatment of the immersed film. These outcomes indicated that some amount of the used ILs as well as formed MR products were released from the film into the water (**Fig. S5**), an interesting characteristic for active packaging and biomedical applications since both ILs and MR products have shown bioactive properties [41,42].

For further assessment, non-water soluble films (Fig. 9 B), ChSer NH, ChAc NH, C10 HT, ChDHP HT, ChSer HT and ChAc HT films, were immersed in PBS at 37 °C for 24 h to simulate physiological conditions. As shown in Fig. 10, only [Ch][Ser]- and [Ch][Ac]-containing HT films kept their integrity after being immersed into body-simulating conditions, while C10 HT and ChDHP HT films, although being non-water soluble, lost their integrity after immersion into PBS at 37 °C. As gelatin presents a relatively low melting temperature (around 30 °C), the sol-gel transition happens at physiological temperature (37 °C), while it is avoided at lower temperatures (23 °C). Therefore, these results indicate that [Ch][Ser] and [Ch][Ac] IL addition, along with the

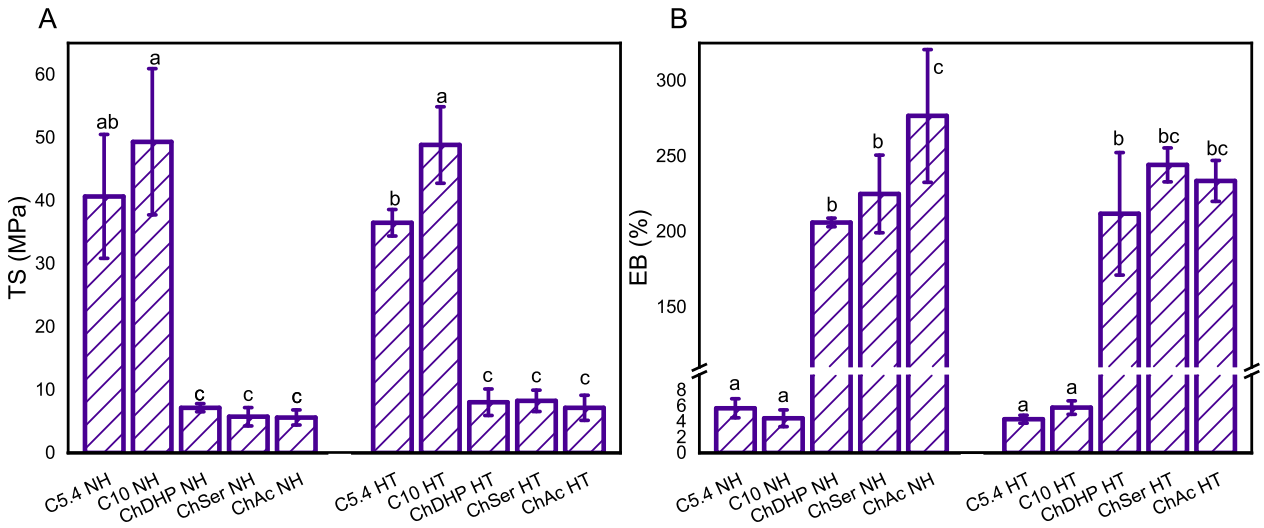


Fig. 7. A) Tensile strength (TS) and B) elongation at break (EB) values for gelatin films as a function of pH (5.4 and 10), addition of ionic liquids ([Ch][DHP], [Ch][Ser] and [Ch][Ac]) and heat treatment (non-heated (NH) and heat-treated (HT)). Means that do not share a letter (a, b, c) are significantly ($p < 0.05$) different ($n = 4$).

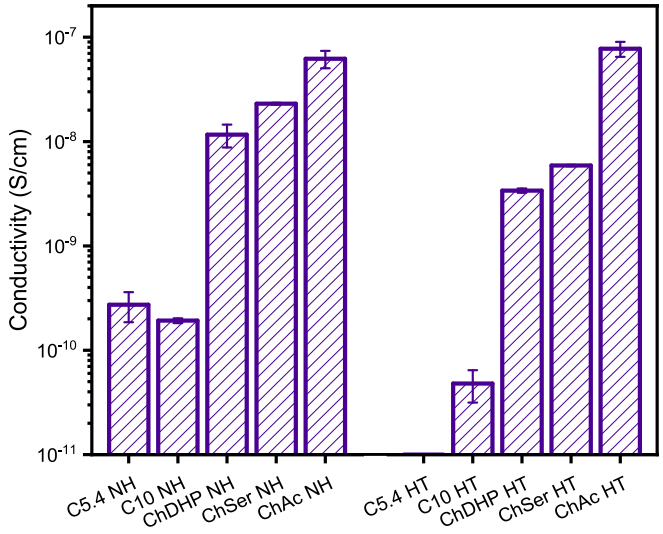


Fig. 8. Electrical conductivity values for gelatin films as a function of pH (5.4 and 10), the addition of ionic liquids ([Ch][DHP], [Ch][Ser] and [Ch][Ac]) and heat treatment (non-heated (NH) and heat-treated (HT)) ($n = 2$).

heat treatment, promoted stronger interactions among gelatin, IL and sugar and that these interactions were capable of standing body-simulant conditions.

3.6. Antimicrobial activity

The non-water soluble films (ChSer NH, ChAc NH, C10 HT, ChDHP HT, ChSer HT and ChAc HT) were assessed in terms of antibacterial activity (Fig. 11). These samples were able to inhibit bacterial growth after 2 h of contact. A strong bacteriostatic effect was observed against *S. aureus*, with nearly all of them showing growth inhibition of around 70 %. ChDHP HT was the most effective film, as it could reduce the bacterial population by about 90 %. Oppositely, the bacteriostatic effect against *E. coli* was negligible. Chen and colleagues [41] observed that the inhibitory effect of MR products on Gram-positive bacteria (*S. aureus*) was significantly higher than that on Gram-negative bacteria (*E. coli*). Similarly, Garcia and co-workers [43] explained that [Ch]-based ILs were more active against Gram-positive bacteria than against Gram-negative bacteria and the lower activity of [Ch]-based ILs against Gram-negative bacteria was ascribed to the lower permeability of their outer membranes. Gram-positive bacteria have a tick cell wall, whereas Gram-negative bacteria have a relatively thin cell wall that is covered by another protective outer membrane. Therefore, it could be said that these films showed potential against Gram-positive bacteria such as *S. aureus*, organisms causing foodborne diseases and persistent infections in chronic wounds [44,45].

3.7. Cytotoxicity

Considering the results of solubility in physiological conditions (Fig. 10), a cytotoxicity evaluation on the L929 cell line was conducted on [Ch][Ser]- and [Ch][Ac]-containing HT films (Fig. 12) to assess their potential for biomedical applications. The results showed cell viability values greater than 70 %, which is the ISO 10993-5 threshold (dotted line in Fig. 12). This indicated that none of the assessed samples was cytotoxic. These results were expected since [Ch]-based IL as well as MR products have shown low cytotoxicity values [46–48].

4. Conclusions

Gelatin films have been prepared through the Maillard reaction and with the addition of choline-based ionic liquids, including [Ch][DHP], [Ch][Ac], and [Ch][Ser]. Films with homogeneous structures and no agglomerations were observed by SEM, indicating good compatibility among all the film-forming components (gelatin, sugar and ILs). The direct (FTIR) and indirect (colour, UV–Vis light absorbance and solubility) measurements of crosslinking showed that physical interactions (e.g. H-bonding and electrostatic interactions) and Maillard reaction (MR) occurred. These interactions induced brownish (a* and b* colour parameter values notably increased), enhanced UV–Vis light absorption and reduced the solubility of the films in food and body simulated conditions, being the effect of MR higher than that of the addition of ILs. The addition of different [Ch]-based ILs significantly improved films' flexibility (from 6 % up to 275 % for elongation at break) and conductivity (up to 7.76×10^{-8} S/cm), whereas their crystallinity was reduced. These changes were related to the plasticising effect of ILs, as well as to the increase in ionic mobile species associated with the IL within the films. Furthermore, the presence of ILs and MR products provided films with a strong bacteriostatic effect against *S. aureus* and the films were not cytotoxic. Among all the films, [Ch][Ser]- and [Ch][Ac]-containing

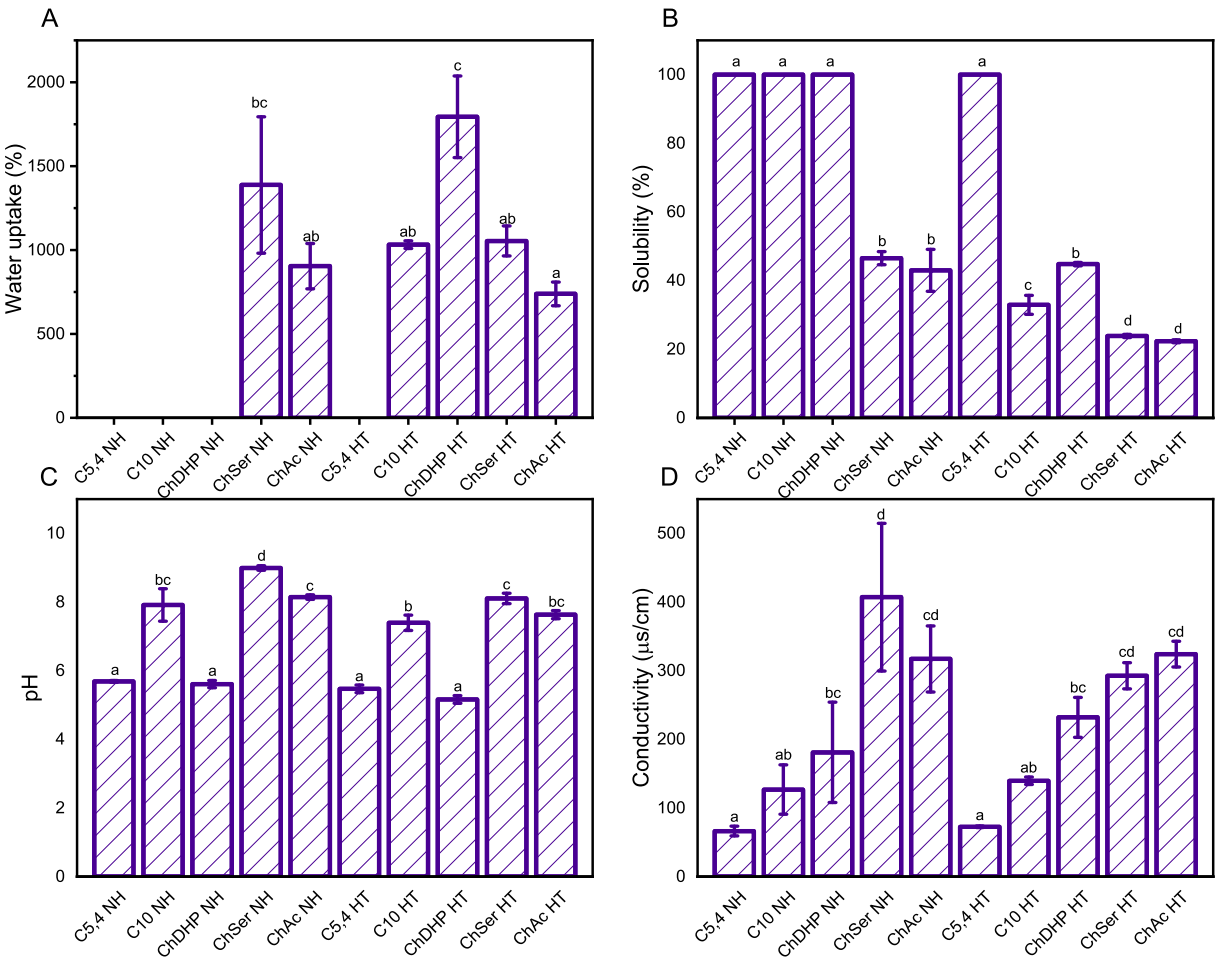


Fig. 9. A) Water uptake and B) water solubility values for gelatin films as a function of pH (5.4 and 10), the addition of ionic liquids ([Ch][DHP], [Ch][Ser] and [Ch][Ac]) and heat treatment (non-heated (NH) and heat-treated (HT)); C) pH and D) conductivity values for water after solubility tests. Means that do not share a letter (a, b, c, d) are significantly ($p < 0.05$) different ($n = 3$).

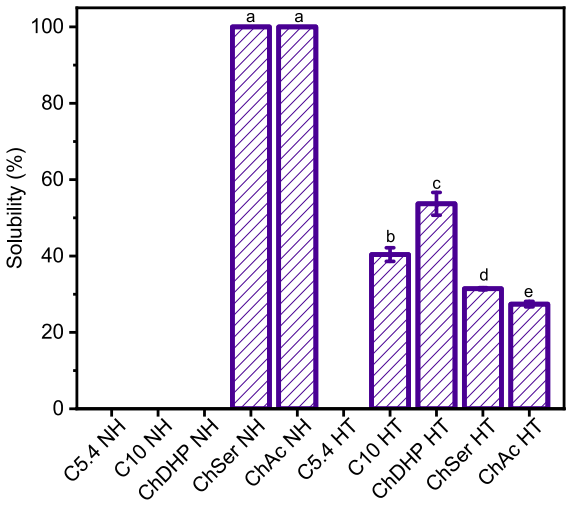


Fig. 10. Solubility in PBS at 37 °C for gelatin-based films as a function of pH (5.4 and 10), the addition of ionic liquids ([Ch][DHP], [Ch][Ser] and [Ch][Ac]) and heat treatment (non-heated (NH) and heat-treated (HT)). Means that do not share a letter (a, b, c, d) are significantly (p < 0.05) different (n = 3).

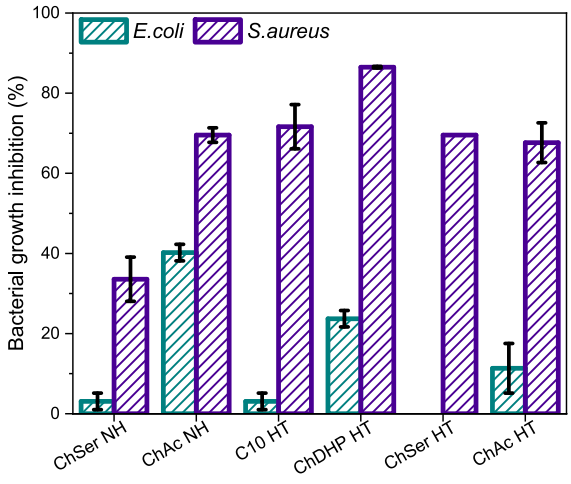


Fig. 11. Bacteriostatic activity against *E. coli* and *S. aureus* of non-water soluble films as a function of pH (5.4 and 10), the addition of ionic liquids ([Ch][DHP], [Ch][Ser] and [Ch][Ac]) and the heat treatment (non-heated (NH) and heat-treated (HT)) ($n = 2$).

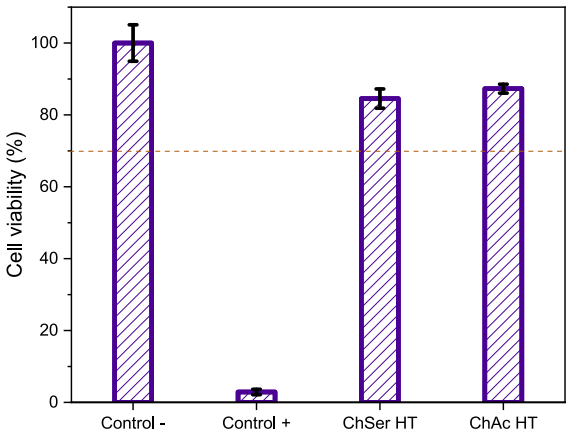


Fig. 12. Cytotoxicity values for heat-treated (HT) gelatin-based films with [Ch][Ser] and [Ch][Ac] ionic liquids.

HT films showed promising outcomes (improved light barrier, conductivity and water stability properties; medium water permeability; antimicrobial properties; no cytotoxicity) to tailor bio-based materials' properties, with the aim of reducing the use of synthetic polymers.

CRediT authorship contribution statement

Alaitz Etxabide: Writing – original draft, Investigation, Formal analysis, Data curation. **Estela O. Carvalho:** Writing – review & editing, Formal analysis, Data curation. **Nelson Pereira:** Writing – review & editing, Formal analysis, Data curation. **Daniela Correia:** Writing – review & editing, Formal analysis, Data curation. **Pedro Guerrero:** Writing – review & editing, Supervision, Resources, Methodology, Investigation. **Carlos M. Costa:** Writing – review & editing, Supervision, Methodology, Investigation. **Koro de la Caba:** Writing – review & editing, Supervision, Project administration, Investigation, Funding acquisition. **Senentxu Lanceros-Mendez:** Writing – review & editing, Supervision, Resources, Investigation, Funding acquisition, Project administration.

Declaration of competing interest

The authors declare that they have no known competing financial interests or personal relationships that could have appeared to influence the work reported in this paper.

Acknowledgements

The authors would like to thank the European Union (H2020_MSCA-RISE-2017 778412 and HORIZON_MSCA-SE-2022 101131379) and the Basque Government (IT1658-22) for their financial support. This work has been supported by PID2022-138572OB-C42 project funded by MCIN/AEI/10.13039/501100011033/FEDER, UE and by the project BIOIMP_ACE_MAS_6_E, co-funded by the European Union through the Interreg VI-A Spain-Portugal Programme (POCTEP) 2021-2027. The authors thank the Fundação para a Ciência e Tecnologia (FCT) for financial Support under the framework of Strategic Funding UIDB/04650/2020, UID/FIS/04650/2020 and UID/EEA/04436/2020, and under projects POCI-01–0247-FEDER-046985, and 10.54499/2022.03931.PTDC, 2022.03931.PTDC funded by national funds through FCT and by the ERDF through the COMPETE2020—Programa Operacional Competitividade e Internacionalização (POCI). The authors also thank the FCT for financial support under FCT investigator 2020.04028.CEECIND (DOI: 10.54499/2020.04028. CEECIND/CP1600/CT0018) (C.M.C.).

Appendix A. Supplementary data

Supplementary data to this article can be found online at https://doi.org/10.1016/j.reactfunctpolym.2025.106445.

Data availability

Data will be made available on request.

References

[1] A. Costa, T. Encarnação, R. Tavares, T. Todo Bom, A. Mateus, Bioplastics: innovation for green transition, Polymers 15 (2023) 517, https://doi.org/10.3390/polym15030517.
[2] I. Shahabi-Ghahfarrokhi, H. Almasi, A. Babaei-Ghazvini, Chapter 3 - characteristics of biopolymers from natural resources, in: Y. Zhang (Ed.), Processing and Development of Polysaccharide-Based Biopolymers for Packaging Applications, Elsevier, 2020, pp. 49–95, https://doi.org/10.1016/B978-0-12-818795-1.00003-4.
[3] C.V. Toniciolli Rigueto, M. Rosseto, I. Alessandretti, R. de Oliveira, D.A. R. Wohlmuth, J. Ferreira Menezes, R.A. Loss, A. Dettmer, I.R. Pizzutti, Gelatin films from wastes: a review of production, characterization, and application trends in food preservation and agriculture, Food Res. Int. 162 (2022) 112114, https://doi.org/10.1016/j.foodres.2022.112114.
[4] S.F. Hosseini, M.C. Gómez-Guillén, A state-of-the-art review on the elaboration of fish gelatin as bioactive packaging: special emphasis on nanotechnology-based approaches, Trends Food Sci. Technol. 79 (2018) 125–135, https://doi.org/10.1016/j.tifs.2018.07.022.
[5] A. Schindl, M.L. Hagen, S. Muzammal, H.A.D. Gunasekera, A.K. Croft, Proteins in ionic liquids: reactions, applications, and futures, Front. Chem. 7 (2019) 347, https://doi.org/10.3389/fchem.2019.00347.
[6] A. Moeini, N. Germann, M. Malinconico, G. Santagata, Formulation of secondary compounds as additives of biopolymer-based food packaging: a review, Trends Food Sci. Technol. 114 (2021) 342–354, https://doi.org/10.1016/j.tifs.2021.05.040.
[7] L.P. Amenorfe, E.S. Agorku, F. Sarpong, R.B. Voegborlo, Innovative exploration of additive incorporated biopolymer-based composites, Sci. Afr. 17 (2022) e01359, https://doi.org/10.1016/j.sciaf.2022.e01359.
[8] A. Etxabide, C. Vairo, E. Santos-Vizcaino, P. Guerrero, J.L. Pedraz, M. Igartua, K. de la Caba, R.M. Hernandez, Ultra thin hydro-films based on lactose-crosslinked fish gelatin for wound healing applications, Int. J. Pharm. 530 (2017) 455–467, https://doi.org/10.1016/j.ijpharm.2017.08.001.
[9] B. Jayachandran, T.N. Parvin, M.M. Alam, K. Chanda, B. Mm, Insights on chemical crosslinking strategies for proteins, Molecules 27 (2022) 8124, https://doi.org/10.3390/molecules27238124.
[10] A. Etxabide, D. Mojío, P. Guerrero, K. de la Caba, J. Gómez-Estaca, Chitin nanowhisker-containing photo-crosslinked antimicrobial gelatin films, Food Hydrocoll. 147 (2024) 109371, https://doi.org/10.1016/j.foodhyd.2023.109371.
[11] A. Etxabide, P.A. Kilmartin, J.I. Maté, S. Prabakar, M. Brimble, R. Naffa, Analysis of advanced glycation end products in ribose-, glucose- and lactose-crosslinked gelatin to correlate the physical changes induced by maillard reaction in films, Food Hydrocoll. 117 (2021) 106736, https://doi.org/10.1016/j.foodhyd.2021.106736.
[12] S. Hill, A.M. Easa, Linking proteins using the maillard reaction and the implications for food processors, in: J. O'Brien, H.E. Nursten, M.J.C. Crabbe, J.M. Ames (Eds.), The Maillard Reaction in Foods and Medicine, Woodhead Publishing, 2005, pp. 133–138, https://doi.org/10.1533/9781845698447.3.133.
[13] Zhigang Lei, Biaohua Chen, Yoon-Mo Koo, Douglas R. MacFarlane, Introduction: Ionic liquids, Chem. Rev. 117 (2017) 6633–6635, https://doi.org/10.1021/acs.chemrev.7b00246.
[14] T.J. Szalaty, Ł. Klapiszewski, T. Jesionowski, Recent developments in modification of lignin using ionic liquids for the fabrication of advanced materials–a review, J. Mol. Liq. 301 (2020) 112417, https://doi.org/10.1016/j.molliq.2019.112417.
[15] J.L. Shamshina, P. Berton, Renewable biopolymers combined with ionic liquids for the next generation of supercapacitor materials, Int. J. Mol. Sci. 24 (2023) 7866, https://doi.org/10.3390/ijms24097866.
[16] S.S. Silva, J.F. Mano, R.L. Reis, Ionic liquids in the processing and chemical modification of chitin and chitosan for biomedical applications, Green Chem. 19 (2017) 1208–1220, https://doi.org/10.1039/C6GC02827F.
[17] B.L. Gadilohar, G.S. Shankarling, Choline based ionic liquids and their applications in organic transformation, J. Mol. Liq. 227 (2017) 234–261, https://doi.org/10.1016/j.molliq.2016.11.136.
[18] A. Etxabide, M. Urdanpilleta, I. Gómez-Arriaran, K. de la Caba, P. Guerrero, Effect of pH and lactose on cross-linking extension and structure of fish gelatin films, React. Funct. Polym. 117 (2017) 140–146, https://doi.org/10.1016/j.reactfunctpolym.2017.04.005.
[19] C. Vilela, M. Kurek, Z. Hayouka, B. Röcker, S. Yildirim, M.D.C. Antunes, J. Nilsen-Nygaard, M.K. Pettersen, C.S.R. Freire, A concise guide to active agents for active food packaging, Trends Food Sci. Technol. 80 (2018) 212–222, https://doi.org/10.1016/j.tifs.2018.08.006.
[20] H. Pan, D. Fan, W. Cao, C. Zhu, Z. Duan, R. Fu, X. Li, X. Ma, Preparation and characterization of breathable hemostatic hydrogel dressings and determination of their effects on full-thickness defects, Polymers 9 (2017) 727, https://doi.org/10.3390/polym9120727.

[21] R. Xu, H. Xia, W. He, Z. Li, J. Zhao, B. Liu, Y. Wang, Q. Lei, Y. Kong, Y. Bai, Z. Yao, R. Yan, H. Li, R. Zhan, S. Yang, G. Luo, J. Wu, Controlled water vapor transmission rate promotes wound-healing via wound re-epithelialization and contraction enhancement, Sci. Rep. 6 (2016) 24596, https://doi.org/10.1038/srep24596.
[22] B.M. Trinh, B.P. Chang, T.H. Mekonnen, The barrier properties of sustainable multiphase and multicomponent packaging materials: a review, Prog. Mater. Sci. 133 (2023) 101071, https://doi.org/10.1016/j.pmatsci.2023.101071.
[23] K. Friess, J.C. Jansen, F. Bazzarelli, P. Izák, V. Jarmarová, M. Kačírková, J. Schauer, G. Clarizia, P. Bernardo, High ionic liquid content polymeric gel membranes: correlation of membrane structure with gas and vapour transport properties, J. Membr. Sci. 415-416 (2012) 801–809, https://doi.org/10.1016/j.memsci.2012.05.072.
[24] S.M. Kamal Mohamed, R. Murali Sankar, M.S. Kiran, S.N. Jaisankar, B. Milow, A. B. Mandal, Facile preparation of biocompatible and transparent silica aerogels as ionogels using choline dihydrogen phosphate ionic liquid, Appl. Sci. 11 (2021) 206, https://doi.org/10.3390/app11010206.
[25] A. Tarannum, N.P. Lobo, J.R. Rao, N.N. Fathima, Are aqueous solutions of choline-based ionic liquid biocompatible cross-linkers for collagen? J. Mol. Liq. 303 (2020) 112654 https://doi.org/10.1016/j.molliq.2020.112654.
[26] A. Mehta, J. Raghava Rao, N.N. Fathima, Electrostatic forces mediated by choline dihydrogen phosphate stabilize collagen, J. Phys. Chem. B 119 (2015) 12816–12827, https://doi.org/10.1021/acs.jpcb.5b07055.
[27] M. Murata, Browning and pigmentation in food through the maillard reaction, Glycoconj. J. 38 (2021) 283–292, https://doi.org/10.1007/s10719-020-09943-x.
[28] Y. Mosleh, W. de Zeeuw, M. Nijemeisland, J.C. Bijleveld, P. van Duin, J.A. Poulis, The structure–property correlations in dry gelatin adhesive films, Adv. Eng. Mater. 23 (2021) 2000716, https://doi.org/10.1002/adem.202000716.
[29] F. Liu, B. Chiou, R.J. Avena-Bustillos, Y. Zhang, Y. Li, T.H. McHugh, F. Zhong, Study of combined effects of glycerol and transglutaminase on properties of gelatin films, Food Hydrocoll. 65 (2017) 1–9, https://doi.org/10.1016/j.foodhyd.2016.10.004.
[30] A. Etxabide, I. Leceta, S. Cabezudo, P. Guerrero, K. de la Caba, Sustainable fish gelatin films: from food processing waste to compost, ACS Sustain. Chem. Eng. 4 (2016) 4626–4634, https://doi.org/10.1021/acssuschemeng.6b00750.
[31] P. Rawat, A.L. Saroj, Effect of ionic liquid on plasticized CS-PVP-NaI based bio-polymer blend electrolytes: structural, thermal, dielectric and ion transport properties study, Mater. Sci. Eng. B 288 (2023) 116215, https://doi.org/10.1016/j.mseb.2022.116215.
[32] A.S.F.M. Asnawi, M.H. Hamsan, S.B. Aziz, M.F.Z. Kadir, J. Matmin, Y.M. Yusof, Impregnation of [emim]Br ionic liquid as plasticizer in biopolymer electrolytes for EDLC application, Electrochim. Acta 375 (2021) 137923, https://doi.org/10.1016/j.electacta.2021.137923.
[33] A. Etxabide, M. Urdanpilleta, P. Guerrero, K. de la Caba, Effects of cross-linking in nanostructure and physicochemical properties of fish gelatins for bio-applications, React. Funct. Polym. 94 (2015) 55–62, https://doi.org/10.1016/j.reactfunctpolym.2015.07.006.
[34] D.M. Correia, L.C. Fernandes, M.M. Fernandes, B. Hermenegildo, R.M. Meira, C. Ribeiro, S. Ribeiro, J. Reguera, S. Lanceros-Méndez, Ionic liquid-based materials for biomedical applications, Nanomaterials 11 (2021) 2401, https://doi.org/10.3390/nano11092401.
[35] I.C. Ferreira, D. Araújo, P. Voisin, V.D. Alves, A.A. Rosatella, C.A.M. Afonso, F. Freitas, L.A. Neves, Chitin-glucan complex – based biopolymeric structures using biocompatible ionic liquids, Carbohydr. Polym. 247 (2020) 116679, https://doi.org/10.1016/j.carbpol.2020.116679.
[36] M.A. Haq, Y. Habu, K. Yamamoto, A. Takada, J. Kadokawa, Ionic liquid induces flexibility and thermoplasticity in cellulose film, Carbohydr. Polym. 223 (2019) 115058, https://doi.org/10.1016/j.carbpol.2019.115058.
[37] M.J. Mehta, A. Kumar, Ionic liquid stabilized gelatin–lignin films: a potential UV-shielding material with excellent mechanical and antimicrobial properties, Chem. Eur. J. 25 (2019) 1269–1274, https://doi.org/10.1002/chem.201803763.
[38] M. Andonegi, D.M. Correia, C.M. Costa, S. Lanceros-Mendez, K.d.l. Caba, P. Guerrero, Tailoring physicochemical properties of collagen-based composites with ionic liquids and wool for advanced applications, Polymer 252 (2022) 124943, https://doi.org/10.1016/j.polymer.2022.124943.
[39] J.C. Dias, D.M. Correia, C.M. Costa, C. Ribeiro, A. Maceiras, J.L. Vilas, G. Botelho, V. de Zea Bermudez, S. Lanceros-Mendez, Improved response of ionic liquid-based bending actuators by tailored interaction with the polar fluorinated polymer matrix, Electrochim. Acta 296 (2019) 598–607, https://doi.org/10.1016/j.electacta.2018.11.049.
[40] D.M. Correia, J.C. Barbosa, C.M. Costa, P.M. Reis, J.M.S.S. Esperança, V. de Zea Bermudez, S. Lanceros-Méndez, Ionic liquid cation size-dependent electromechanical response of ionic liquid/poly(vinylidene fluoride)-based soft actuators, J. Phys. Chem. C 123 (2019) 12744–12752, https://doi.org/10.1021/acs.jpcc.9b00868.
[41] X. Chen, D. Jiang, P. Xu, Z. Geng, G. Xiong, Y. Zou, D. Wang, W. Xu, Structural and antimicrobial properties of maillard reaction products in chicken liver protein hydrolysate after sonication, Food Chem. 343 (2021) 128417, https://doi.org/10.1016/j.foodchem.2020.128417.
[42] K.N. Ibsen, H. Ma, A. Banerjee, E.E.L. Tanner, S. Nangia, S. Mitragotri, Mechanism of antibacterial activity of choline-based ionic liquids (CAGE), ACS Biomater Sci. Eng. 4 (2018) 2370–2379, https://doi.org/10.1021/acsbiomaterials.8b00486.
[43] M.T. García, E. Bautista, A. de la Fuente, L. Pérez, Cholinium-based ionic liquids as promising antimicrobial agents in pharmaceutical applications: surface activity, antibacterial activity and ecotoxicological profile, Pharmaceutics 15 (2023) 1806, https://doi.org/10.3390/pharmaceutics15071806.
[44] M. AL-Mamun, T. Chowdhury, B. Biswas, N. Absar, Chapter 11 - food poisoning and intoxication: A global leading concern for human health, in: A.M. Grumezescu, A.M. Holban (Eds.), Food Safety and Preservation, Academic Press, 2018, pp. 307–352, https://doi.org/10.1016/B978-0-12-814956-0.00011-1.
[45] S. Roy, S. Santra, A. Das, S. Dixith, M. Sinha, S. Ghatak, N. Ghosh, P. Banerjee, S. Khanna, S. Mathew-Steiner, P.D. Ghatak, B.N. Blackstone, H.M. Powell, V. K. Bergdall, D.J. Wozniak, C.K. Sen, *Staphylococcus aureus* biofilm infection compromises wound healing by causing deficiencies in granulation tissue collagen, Ann. Surg. 271 (2020) 1174–1185. https://journals.lww.com/annalsofsurgery/fulltext/2020/06000/staphylococcus_aureus_biofilm_infection.29.aspx.
[46] A.Q. Le, V.P. Dang, N.D. Nguyen, C.T. Nguyen, Q.H. Nguyen, Antibacterial activity against *escherichia coli* and cytotoxicity of maillard reaction product of chitosan and glucosamine prepared by gamma co-60 ray irradiation, Polymers 15 (2023) 4397, https://doi.org/10.3390/polym15224397.
[47] J.M. Gomes, S.S. Silva, R.L. Reis, Exploring the use of choline acetate on the sustainable development of α-chitin-based sponges, ACS Sustain. Chem. Eng. 8 (2020) 13507–13516, https://doi.org/10.1021/acssuschemeng.0c05076.
[48] T. Santos de Almeida, A. Júlio, N. Saraiva, A.S. Fernandes, M.E.M. Araújo, A. R. Baby, C. Rosado, J.P. Mota, Choline- versus imidazole-based ionic liquids as functional ingredients in topical delivery systems: cytotoxicity, solubility, and skin permeation studies, Drug Dev. Ind. Pharm. 43 (2017) 1858–1865, https://doi.org/10.1080/03639045.2017.1349788.